

Map representation of the time-delayed system in the presence of Delay Time Modulation: an Application to the stability analysis

Won-Ho Kye¹, Muhan Choi¹, Tae-Yoon Kwon^{1,2}, and Chil-Min Kim¹

¹National Creative Research Initiative Center for Controlling Optical Chaos, Pai-Chai University, Daejeon 302-735, Korea

Young-Jai Park²

²Department of Physics, Sogang University, Seoul 121-742, Korea

We introduce the map representation of a time-delayed system in the presence of delay time modulation. Based on this representation, we find the method by which to analyze the stability of that kind of a system. We apply this method to a coupled chaotic system and discuss the results in comparison to the system with a fixed delay time.

PACS numbers: 05.45.Xt, 05.40.Pq

In a real situation, time delay is inevitable, since the propagation speed of an information signal is finite. The effects of time delay have been investigated in various fields in a form of delay differential equation [1, 2, 3, 4, 5, 6]:

$$\dot{x} = F(x(t), x(t - \bar{\tau})), \quad (1)$$

where $\bar{\tau}$ is the delay time. Since the Volterra's predator-prey model [1], delay time has been considered such various forms as fixed [3, 4, 5, 6], distributed[7], state-dependent [8], and time-dependent [8, 9, 10] ones. Up to now, the delay effects of these forms in dynamical systems have been extensively studied not only in various fields of physics[4], biology [3], and economy [8] but also for the cases of application [2, 11, 12]. The recent discovery [6] that the neural synchrony is enhanced by the discrete time delays shows the delay feedbacks play a significant role in synchronization phenomenon. This discovery calls new scientific attention on the time-delay feedbacks and synchronization phenomenon.

Meanwhile, in regard to the application of time-delayed systems to communication, delay time modulation (DTM) [9, 10, 13, 14] driven by the signal of an independent system was introduced to erase the imprint of the fixed delay time. It was reported that the DTM increases the complexity of the time-delayed system as well as prevents the system from being collapsed into the simple manifold in reconstructed phase space, which was a serious drawback of the time-delayed system to the application to communication. It was also found that the synchronization in the presence of DTM can be established and the death phenomenon is enhanced, due to DTM[10, 13].

It was further shown that the time-delayed system can be represented by high dimensional coupled maps [15] and the methods by which to understand the characteristics of the time delayed system with discrete time delays have been developed [2]. Accordingly, the natural questions to be tackled have become "how can we find the coupled-map representation of the time-delayed system in the presence of DTM?" and "how can we analyze the stability of that kind of system?". The answers on these

two questions are quite essential to understand the synchronization and the enhancement of death phenomenon mentioned above with regard to DTM [10, 13]. In this paper, we newly introduce the coupled-map representation of a time-delayed system in the presence of DTM, and develop a method which enables us to get the Lyapunov exponents of the system based on the representation. We shall also show the DTM accelerates the transition to hyperchaos in a coupled time-delayed system by presenting the Lyapunov spectrum obtained by the method.

The delay differential equation of Eq. (1) can be rewritten by the discrete form:

$$x_{n+1} = f(x_n, x_{n-\tau}), \quad (2)$$

where x_n is the value of x at n -th time step such that $x_n = x(n\Delta t)$ and $x_{n-\tau} = x(n\Delta t - \tau\Delta t)$. Here $f(x_n, x_{n-\tau}) = x(n\Delta t) + F(x(n\Delta t), x(n\Delta t - \tau\Delta t))\Delta t$. It is known that the above system is equivalent to the $(\tau+1)$ dimensional coupled maps [15]:

$$\begin{aligned} x_{n+1}^0 &= f(x_n^0, x_n^\tau), \\ x_{n+1}^\tau &= x_n^{\tau-1}, \\ x_{n+1}^{\tau-1} &= x_n^{\tau-2}, \\ &\vdots \\ x_{n+1}^1 &= x_n^0, \end{aligned} \quad (3)$$

where the variables x_n^1, \dots, x_n^τ construct the "echo type" feedback loop. The above representation plays an important role in analyzing the time-delayed system with fixed delay times. DTM [9] consists of a modulation system, $\dot{y} = G(y)$ which generates the driving signal y_n , and a scaling system, $\bar{\tau} = H(y)$ which adjusts the amplitude of modulation. Accordingly two additional equations are introduced:

$$\begin{aligned} y_{n+1} &= g(y_n), \\ \tau &= h(y_n), \end{aligned} \quad (4)$$

where $g(y_n) = y(n\Delta t) + G(y(n\Delta t))$ and $h(y_n) = H(y(n\Delta t))$. The modulated delay time τ in Eq. (4)

selects the length of delay time for a feedback variable $x_{n-\tau}$. As shown in Eq. (3) the feedback variable (say x_n^τ) is not changed in the fixed delayed system. However, in the time-dependent delayed system, we can interpret that the feeding variable is selected according to the delay time (say x_n^k with $k = 0, 1, 2, \dots, \tau_m$) in Eq. (3). Therefore we introduce the map representation as follows:

$$\begin{aligned} x_{n+1}^0 &= f(x_n^0, x_n^k), \\ x_{n+1}^{\tau_m} &= x_n^{\tau_m-1}, \\ &\vdots \\ x_{n+1}^1 &= x_n^0, \end{aligned} \quad (5)$$

$$\begin{aligned} k &= h(y_n), \\ y_{n+1} &= g(y_n), \end{aligned} \quad (6)$$

where τ_m is the maximum of the amplitude of DTM and k is an integer number which determines the variable to be fed into the systems. We have $R^{\tau_m+1} \times I \times R^1$ phase space. From Eq. (5) and (6), we get the Jacobian matrix as follows:

$$\mathbf{J} = \begin{bmatrix} \frac{\partial f(x_n^0, x_n^k)}{\partial x_n^0} & \frac{\partial f(x_n^0, x_n^k)}{\partial x_n^k} \delta_k^{\tau_m} & \frac{\partial f(x_n^0, x_n^k)}{\partial x_n^k} \delta_k^{\tau_m-1} & \frac{\partial f(x_n^0, x_n^k)}{\partial x_n^k} \delta_k^{\tau_m-2} & \dots & \frac{\partial f(x_n^0, x_n^k)}{\partial x_n^k} \delta_k^1 & \frac{\partial f(x_n^0, x_n^k)}{\partial k} & 0 \\ 0 & 0 & 1 & 0 & \dots & 0 & 0 & 0 \\ 0 & 0 & 0 & 1 & \dots & 0 & 0 & 0 \\ \dots & \dots & \dots & \dots & \dots & \dots & \dots & \dots \\ 0 & 0 & 0 & 0 & \dots & 1 & 0 & 0 \\ 1 & 0 & 0 & 0 & \dots & 0 & 0 & 0 \\ 0 & 0 & 0 & 0 & \dots & 0 & 0 & \frac{\partial h(y_n)}{\partial y_n} \\ 0 & 0 & 0 & 0 & \dots & 0 & 0 & \frac{\partial g(y_n)}{\partial y_n} \end{bmatrix}, \quad (7)$$

where $\delta_k^l = 1$ only if $k = l$ else $\delta_k^l = 0$. We introduce the $(\tau_m + 3)$ dimensional orthonormalized initial vectors such that: $\hat{\mathbf{y}}_1 = (1, 0, 0, \dots)$, $\hat{\mathbf{y}}_2 = (0, 1, 0, \dots)$, and \dots which are evolved by $\hat{\mathbf{y}}'_i = \mathbf{J}\hat{\mathbf{y}}_i$. By following the standard procedure [16], we can find the Lyapunov spectrum of the time-delayed system in the presence of DTM as follows:

$$\lambda_i = \frac{1}{rT} \sum_{k=1}^r \ln N_i^k, \quad (8)$$

where r is the number of orthonormalization within the chosen finite time interval T and N_i^k is the norm of the i -th vector at k -th orthonormalization process.

As an example of DTM, we consider the two coupled logistic maps as follows:

$$\begin{aligned} x_{n+1} &= \gamma \bar{x}_n^\tau (1 - \bar{x}_n^\tau), \\ \tau &= [\Lambda y_n], \\ y_{n+1} &= \gamma_0 y_n (1 - y_n), \end{aligned} \quad (9)$$

Here $\bar{x}_n^\tau = (1 - \alpha)x_n + \alpha(x_{n-\tau})$ and α is a coupling

strength. We took $\gamma_0 = 4.0$ and $\Lambda = 4.0$ and $[x]$ denotes the maximum of the integer which is less than x and $\tau_m = \max([\Lambda y_n]) = 3$. According to the general representation of Eqs. (5) and (6), the system described in Eq. (9) can be rewritten by the 6-dimensional coupled maps as follows:

$$\begin{aligned} x_{n+1}^0 &= \gamma \bar{x}_n^k (1 - \bar{x}_n^k) \equiv F(\bar{x}_n^k), \\ x_{n+1}^3 &= x_n^2, \\ x_{n+1}^2 &= x_n^1, \\ x_{n+1}^1 &= x_n^0, \end{aligned} \quad (10)$$

$$\begin{aligned} k &= [\Lambda y_n], \\ y_{n+1} &= \gamma_0 y_n (1 - y_n), \end{aligned} \quad (11)$$

where $\bar{x}_n^k = (1 - \alpha)x_n^0 + \alpha x_n^k$. The corresponding Jacobian matrix is given by:

$$\mathbf{J} = \begin{bmatrix} \gamma((1-\alpha) + \alpha\beta\delta_0^k)(1-2\bar{x}_n^k) & \gamma\alpha\delta_3^k(1-2\bar{x}_n^k) & \gamma\alpha\delta_2^k(1-2\bar{x}_n^k) & \gamma\alpha\delta_1^k(1-2\bar{x}_n^k) & F(\bar{x}_n^{k+1}) - F(\bar{x}_n^k) & 0 \\ 0 & 0 & 1 & 0 & 0 & 0 \\ 0 & 0 & 0 & 1 & 0 & 0 \\ 1 & 0 & 0 & 0 & 0 & 0 \\ 0 & 0 & 0 & 0 & 0 & 0 \\ 0 & 0 & 0 & 0 & 0 & \gamma_0(1-2y_n) \end{bmatrix}, \quad (12)$$

where we have used the relation $\frac{\partial F(x_n^0, x_n^k)}{\partial k} = F(x_n^0, x_n^{k+1}) - F(x_n^0, x_n^k)$ noting that k is an integer [17] and Here $\frac{\partial[\Delta y_n]}{\partial y_n}$ is not zero only at 0.25, 0.50, and 0.75 which are unstable periodic orbits of the driving logistic map (the second equation of Eq. (11)). Therefore we put $\frac{\partial[\Delta y_n]}{\partial y_n} = 0$ to the above equation.

To verify our method, we calculate the Lyapunov spectrum in the case of DTM as well as in the fixed delay case. We can easily restore Eq. (10) to the fixed delay case by fixing $k = 3$ without Eq. (11). One can see the bifurcation diagram presented in Fig. 1 (a) and the corresponding Lyapunov spectrum in Fig. 1 (c). The quasi-periodic regime in $\gamma \in [3.1, 3.7]$ and the periodic window in $\gamma \in [3.7, 3.8]$ are exactly matched with the corresponding Lyapunov spectra. As one can see, the bifurcation diagram is different from that of the single logistic map, which is due to the delay feedback [15]. In the case of fixed delay (Fig. 1 (a) and (c)), two largest Lyapunov exponents become positive above $\gamma = 3.8$ through the quasi-periodic regime in $\gamma \in [3.1, 3.7]$. That is to say, the system develops to hyperchaos above that point.

The Lyapunov exponents in the case of DTM are presented in Fig. 1 (d). Actually we have two more Lyapunov exponents which are not plotted in the figure. One has a constant value, $\lambda_5 = 0.691 \dots$, which describes the dynamics of isolated master system and the other has a relatively large negative value, $\lambda_6 \in [-0.5, -0.6]$. While in fixed delay time, x_n^τ is directly fed into the delayed system, in DTM all delay variables $x_n^0, x_n^1, \dots, x_n^\tau$ can contribute to the system depending on the state of the modulating signal y_n . For this reason, the largest Lyapunov exponents are very closer with each other (Fig. 1 (c)) than those of the fixed delay time (Fig. 1 (d)). The sum of positive Lyapunov exponents $\sum_{\lambda_i > 0} \lambda_i$ is the entropy of the system which quantifies the complexity of the system [18]. For example, at $\gamma = 3.95$ the sum of positive

Lyapunov exponents is 0.262 in the case of DTM, while it is 0.128 in the case of fixed delay time. This type of behavior caused by DTM is fulfilled with the result of the recent report in which the entropy is increased depending on the property of the driving signal for DTM [14].

Figure 2 (a) shows the time series at the intermittent regime ($\gamma = 3.5$) and (b) shows the time series at the hyperchaotic regime ($\gamma = 3.95$) when the delay is modulated. The return maps are presented in Fig. 2 (c) and (d), which show a complex structure. Comparing the correlation functions in Fig. 2 (e) (with the fixed delay time) and (f) (with DTM), one is confirmed that the DTM reduces the length of correlation [10]. We emphasize that all the procedure can be applied to another system regardless of coupled maps or flows in principle because in case of flow, the system also can be represented by the same form of coupled maps of Eqs. (5) and (6) (one just needs to note that the dimension of the phase space is determined by the value of delay time τ and the chosen time step Δt such that $\dim \sim \tau/\Delta t$).

In conclusion, we have introduced the coupled-map representation of the time-delayed system in the presence of delay time modulation and found the method by which to analyze the stability of the system. We have applied this method to a coupled chaotic system and confirmed that the Lyapunov spectrum of the time-delayed system in the presence of DTM can be exactly determined which explains the bifurcation behavior. Furthermore, we have observed that DTM erases the preference of the feedback variable, by scanning all delay variables during the evolution, and that for this reason it leads Lyapunov exponents to be close to each other.

The authors thank M.S. Kurdoglyan and K. V. Volodchenko for valuable discussions. This work is supported by Creative Research Initiatives of the Korean Ministry of Science and Technology.

-
- [1] V. Volterra, *Lecons sur la théorie mathématique de la lutte pour la vie* (Gauthiers-Villars, Paris, 1931).
[2] K. Pyragas, Phys. Rev. Lett. **86**, 2265 (2001); O. Lüthje, S. Wolf, and G. Pfister, Phys. Rev. Lett. **86**, 1745 (2001).
[3] J. Fort and V. Méndez, Phys. Rev. Lett. **89**, 178101 (2002).
[4] T. Heil, I. Fischer, W. Elsässer, J. Mulet, and C. R. Mi-

- rosso, Phys. Rev. Lett. **86**, 795 (2001).
[5] J.D. Farmer, Physica D **4**, 366 (1982); K.M. Short and A.T. Parker, Phys. Rev. E **58**, 1159 (1998).
[6] M. Dhamala, V.K. Jirsa, and M. Ding, Phys. Rev. Lett. **92**, 074104 (2004).
[7] F. Ghiringhelli and M. N. Zervas, Phys. Rev. E **65**, 036604 (2002); F.M. Atay, Phys. Rev. Lett. **91**, 094101

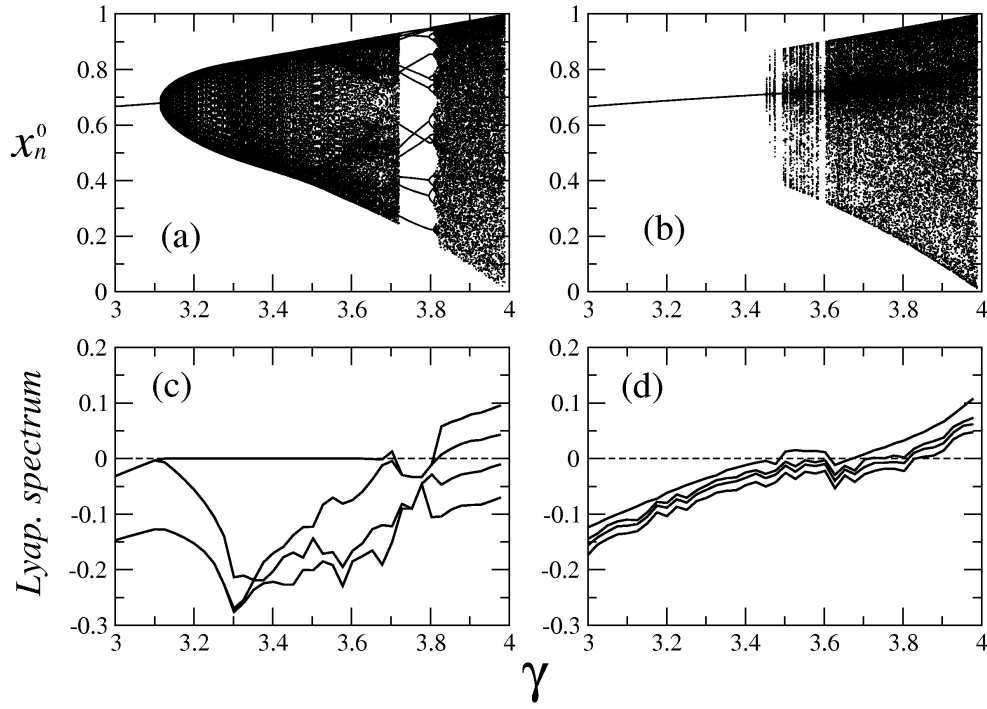


FIG. 1: The bifurcation diagrams and the Lyapunov spectra with $\alpha = 0.7$. (a) and (c) show the bifurcation diagram and Lyapunov spectra at fixed delay time (only using Eq. (10) with $k = \tau_m$), (b) and (d) at DTM (using Eq. (10) and (11)). We have taken $r = 5000$ orthonormalization process with the period of $T = 70$ for each point (see Eq. (8)).

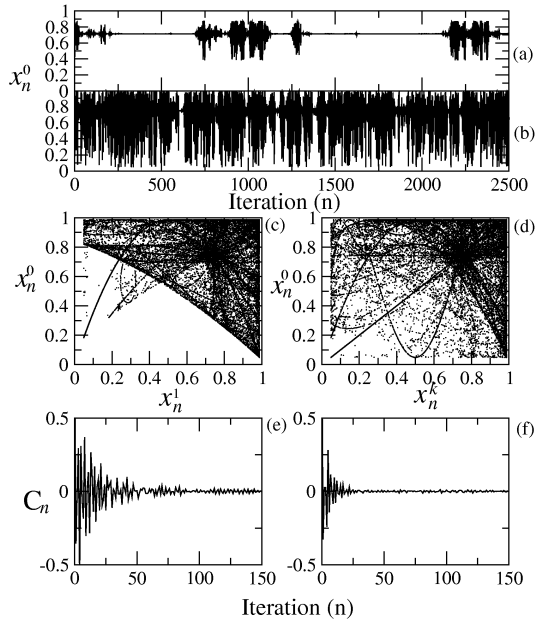


FIG. 2: Temporal behaviors and retrun maps of delayed logistic map in the presence of DTM (Eq. (10) and (11)). (a) Time series of x_n^0 at $\gamma = 3.5$ (b) at $\gamma = 3.95$; (c) return map x_n^0 versus x_n^1 (d) x_n^0 versus x_n^k ; autocorrelation functions of x_n^0 as a function of iteration at $\gamma = 3.95$ in cases of (e) fixed delay and (f) DTM.

- (2003).
- [8] J.K. Hale, *Theory of Functional Differential Equations*, Springer-Verlag, Berlin, (1997) and references therein; W. Alt, *Lecture Notes Math.* 730, 16-31 (1979); J. Bélair, *Lecture notes in pure and Applied Mathematics*, Vol. 131, Marcel Dekker, 165-176 (1991).
- [9] S. Madrugá, S. Boccaletti, M.A. Matias, *Int. J. Bifur. Chaos* **11**, 2875 (2001).
- [10] W.-H. Kye, M. Choi, M.-W. Kim, S.-Y. Lee, S. Rim, C.-M. Kim, Y.-J. Park, *Phys. Lett. A* 322, 338 (2004).
- [11] R. He and P.G. Vaidya, *Phys. Rev. E* **59**, 4048 (1999); L. Yaowen, G. Gguangming, Z. Hong, and W. Yinghai, *Phys. Rev. E* **62**, 7898 (2000).
- [12] V.S. Udaltsov, J.-P. Goedgebuer, L. Larger, and W.T. Rhodes, *Phys. Rev. Lett.* **86**, 1892 (2001).
- [13] W.-H. Kye, C.-M. Kim, M. Choi, M.-W. Kim, S. Rim, S. Lee, Y.-J. Park, submitted to *Phys. Rev. E* (2004).
- [14] W.-H. Kye, M. Choi, S. Rim, M.S. Krudoglyan, C.-M. Kim, Y.-J. Park, *Phys. Rev. E* **69**, (in press) (2004).
- [15] F.T. Arecchi, G. Giacomelli, A. Lapucci, and R. Meucci, *Phys. Rev. E* **45**, R4225 (1992); T. Buchner and J.I. Zebrowski, *Phys. Rev. E* **63**, 016210 (2000).
- [16] Ali H. Nayfeh and B. Balachandran, *APPLIED NON-LINEAR DYNAMICS Analytical, Computational, and Experimental Methods*, 1995, John Wiley & Sons, New York.
- [17] Alternatively, using the chain rule, we can use the relation $\frac{\partial F(x_n^0, x_n^k)}{\partial k} = \frac{\partial F(x_n^0, x_n^k)}{\partial x_n^k} \frac{\partial x_n^k}{\partial k} = \frac{\partial F(x_n^0, x_n^k)}{\partial x_n^k} (x_n^{k+1} - x_n^k)$. We confirmed that the Lyapunov spectrum is the same within the error bound of the order $\sim 10^{-4}$.
- [18] H.D.I. Abarbanel, *Analysis of Observed Chaotic Data*,

1996 Springer-Verlag New York.